

Structural Organization of Parallel Information Processing Within the Tectofugal Visual System of the Pigeon

BURKHARD HELLMANN* AND ONUR GÜNTÜRKÜN

Ruhr-Universität Bochum, Fakultät für Psychologie, AE Biopsychologie,
44780 Bochum, Germany

ABSTRACT

Visual information processing within the ascending tectofugal pathway to the forebrain undergoes essential rearrangements between the mesencephalic tectum opticum and the diencephalic nucleus rotundus of birds. The outer tectal layers constitute a two-dimensional map of the visual surrounding, whereas nucleus rotundus is characterized by functional domains in which different visual features such as movement, color, or luminance are processed in parallel. Morphologic correlates of this reorganization were investigated by means of focal injections of the neuronal tracer cholera toxin subunit B into different regions of the nuclei rotundus and triangularis of the pigeon. Dependent on the thalamic injection site, variations in the retrograde labeling pattern of ascending tectal efferents were observed. All rotundal projecting neurons were located within the deep tectal layer 13. Five different cell populations were distinguished that could be differentiated according to their dendritic ramifications within different retinorecipient laminae and their axons projecting to different subcomponents of the nucleus rotundus. Because retinorecipient tectal layers differ in their input from distinct classes of retinal ganglion cells, each tectorotundal cell type probably processes different aspects of the visual surrounding. Therefore, the differential input/output connections of the five tectorotundal cell groups might constitute the structural basis for spatially segregated parallel information processing of different stimulus aspects within the tectofugal visual system. Because two of five rotundal projecting cell groups additionally exhibited quantitative shifts along the dorsoventral extension of the tectum, data also indicate visual field-dependent alterations in information processing for particular visual features. *J. Comp. Neurol.* 429:94–112, 2001. © 2001 Wiley-Liss, Inc.

Indexing terms: tectum opticum; nucleus rotundus, functional parcellation; extrageniculocortical pathway; birds

In pigeons, approximately 90% of retinal ganglion cells contribute to the tectofugal pathway, which is homologous to the extrageniculocortical system in mammals (Shimizu and Karten, 1993). Within the tectofugal pathway, visual input ascends from the mesencephalic tectum opticum, via the diencephalic nucleus rotundus to the telencephalic ectostriatum (Benowitz and Karten, 1976). Tectal, rotundal, or ectostriatal lesions result in severe deficits in intensity, color, pattern, acuity, or movement discrimination (Hodos and Karten, 1966; Hodos, 1969; Hodos and Bonbright, 1974; Mulvanny, 1979; Hodos et al., 1984; Macko and Hodos, 1984; Bessette and Hodos, 1989; Watanabe, 1991; Güntürkün and Hahmann, 1999). The deficits in pattern discrimination tasks and the dramatic postlesional threshold elevations in acuity measurements especially suggest the existence of a neural system with high spatial resolution.

Indeed, the outer retinorecipient layers of the tectum are characterized by a precise retinotopic representation with narrowly tuned receptive fields of less than 1° (Hamdi and Whitteridge, 1954; Jassik-Gerschenfeld and Hardy, 1984). However, receptive field widths gradually increase in deeper tectal layers (Jassik-Gerschenfeld and Guichard, 1972) to finally span up to 180° (Frost and

Grant sponsor: Deutsche Forschungsgemeinschaft; Grant numbers: Gu 227/4-3 and Sonderforschungsbereich 509 NEUROVISION; Grant sponsor: the Alfried Krupp-Stiftung.

*Correspondence to: Burkhard Hellmann, AE Biopsychologie, Fakultät für Psychologie, Ruhr-Universität Bochum, 44780 Bochum, Germany. E-mail: burkhard.hellmann@ruhr-uni-bochum.de

Received 27 June 2000; Revised 8 September 2000; Accepted 8 September 2000

DiFranco, 1976) in neurons of the efferent tectal layer 13 neurons, which are the exclusive source of the ascending projection to nucleus rotundus (Karten and Revzin, 1966). Although layer 13 neurons probably receive direct input from retinal terminals in superficial tectal layers, they sample retinal input with their extensive dendritic arbors from such a wide tectal area that detailed topographic information is probably lost (Ramon y Cajal, 1995; Hunt and Künzle, 1976; Hunt and Brecha, 1984; Karten et al., 1997; Luksch et al., 1998). Indeed, retinotopic place coding seems to be absent within nucleus rotundus, because each point of the tectum is connected to nearly the entire rotundus and its dorsal cap, the nucleus triangularis (Benowitz and Karten, 1976; Nixdorf and Bischof, 1982; Ngo et al., 1994; Deng and Rogers, 1998; Hellmann and Gütürkün, 1999). Instead of retinotopy, a new functionally based segregation seems to take place in the thalamus, because electrophysiologic data could demonstrate functional rotundal domains (Granda and Yazulla, 1971; Jassik-Gerschenfeld and Guichard, 1972; Yazulla and Granda, 1973; Frost and DiFranco, 1976; Revzin, 1979; Wang and Frost, 1992) in which mainly color, luminance, motion, or looming are processed (Wang et al., 1993). Behavioral data support this view because restricted rotundal lesions were shown to affect performance in only specific aspects of visual analysis (Laverghetta and Shimizu, 1999). In contrast to the tectorotundal connection, the rotundoectostriatal projection (Benowitz and Karten, 1976; Nixdorf and Bischof, 1982) as well as subsequent secondary and tertiary connections within the forebrain (Husband and Shimizu, 1999) are organized topographically, suggesting rotundal functional segregation to be carried on within the forebrain.

Thus, the tectofugal system is transformed at the tectal level from a retinotopically organized system with small receptive fields into a pathway that is composed of functionally segregated entities made up of neurons encompassing wide receptive fields. Understanding the functional architecture of the tectofugal visual pathway requires an answer to the key question how visual images are preserved and transformed at the tectorotundal junction. Therefore, the aim of the present study was to perform a detailed analysis of the tectorotundal projection to understand the structural basis of this transformation.

MATERIALS AND METHODS

Twenty-five adult pigeons (*Columba livia*) of both sexes from local breeding stocks received injections of the neuronal tracer cholera toxin subunit B (CtB; Sigma, Deisenhofen, Germany) into the left diencephalic nucleus rotundus (RT) or left nucleus triangularis (T). All experiments were carried out according to the specifications of the German law for the prevention of cruelty to animals.

Before surgery, the pigeons were anesthetized with equithesin (0.31–0.33 ml/100 g body weight) and the animals were placed into a stereotaxic apparatus (Karten and Hodos, 1967). The scalps were infiltrated with lidocaine (Xylocaine) and were incised dorsally. Next, the skull was opened with a dental drill, and a glass micropipette (outer tip diameter 20 μ m) mounted to a mechanical pressure device (WPI Nanoliterinjector, WPI, USA) was inserted into varying sites of the left RT or T (anterior 5.3–7.0, dorsal 5.0–7.2, lateral 1.8–3.8) according to stereotaxic coordinates of the pigeon brain atlas by Karten and Hodos (1967). Thirty-four nanoliters CtB [1%

(wt/vol) in distilled water] were injected in steps of 2 nl during a 15–20 min period. Subsequently, the pipette was removed, and the skin was infiltrated again with lidocaine and sutured.

After 2 days' survival time, animals received an injection of 200 U sodium heparin and were then deeply anesthetized with an overdose of equithesin (0.55 ml/100 g body weight). The pigeons were perfused through the heart with 100 ml 0.9% (wt/vol) sodium chloride and 800 ml ice-cold 4% paraformaldehyde in 0.12 M phosphate buffer (PB), pH 7.4. The brains were removed and stored for 2 hours in fixative with supplement of 15% sucrose (wt/vol). Subsequently, the brains were stored overnight in a solution of 30% sucrose in 0.12 M PB. On the following day, the brains were cut in frontal plane at 35 μ m on a freezing microtome and the slices were collected in PB containing 0.1% sodium azide (wt/vol).

Brain slices were reacted free-floating according to the immuno-ABC-technique. The sections were placed for 35 minutes in 0.5% hydrogen peroxidase in distilled water to reduce endogenous peroxidase activity. After rinsing, sections were incubated overnight at 4°C in the primary antibody [rabbit anti-Cholera toxin subunit B; Sigma, Germany; 1/20,000 in 0.12 M PB with the addition of 2% NaCl (wt/vol), 0.3% Triton-X-100 (vol/vol) and 5% normal goat serum]. After being rinsed, the sections were incubated for 60 minutes at room temperature in the biotinylated secondary antibody [goat anti-rabbit; Vectastain, Vector, Camon (Wiesbaden, Germany); 1/250 in 0.12 M PB + 2% NaCl + 0.3% Triton-X-100]. After additional rinsing, the sections were incubated for 60 minutes in avidin-biotin-peroxidase solution (Vectastain ABC-Elite kit, Vector, Camon; 1/100 in 0.12 M PB + 2% NaCl + 0.3% Triton-X-100). After washing, the peroxidase activity was detected using a heavy metal intensified 3',3'-diaminobenzidine (Sigma) reaction (Adams, 1981), modified by the use of β -D-glucose/glucose-oxidase (Sigma) instead of hydrogen peroxidase (Shu et al., 1988). The sections were mounted on gelatin-coated slides, dehydrated, and coverslipped with DPX (Fluka, Neu-Ulm, Germany) or Permount (Fischer Scientific, Fair Lawn, NJ). Some sections were counterstained with cresyl violet.

The rotundal tracer injection sites and the resulting retrograde CtB labeling within the tectum opticum, nucleus subpretectalis (SP), nucleus interstitionipretectosubpretectalis (IPS), and nucleus of the tractus tectothalamicus (nTT) were analyzed using an Olympus BH2 microscope. Qualitative reconstruction of rotundal/triangular CtB diffusion area and the location of labeled somata as well as their peripheral processes were made in Nissl counterstained sections. Drawings were performed using digitized microscopic images [JVC-TK C1381 and GrabitPCI grabber (SIS, Münster, Germany) in PC-software Designer 3.1 (Micrografix, Dallas, TX)]. Quantitative determinations of soma size, number, and distribution were performed in digitized images with the help of an image analyzing system (analySIS 3.0 Doku, SIS) in 10 pigeons. The number of retrogradely labeled layer 13 somata was estimated within the ipsilateral as well as contralateral tectum along a rostrocaudal extent of 2.8 mm (A 1.5–A 4.3; Karten and Hodos, 1967) by counting CtB-labeled cells in every 10th section with 450 \times magnification. The soma size of layer 13 neurons in the dorsal (100 cells) and the ventral ipsilateral tectum (100 cells) was measured at A 3.0 (overall magnification 1,800 \times). Dorso-

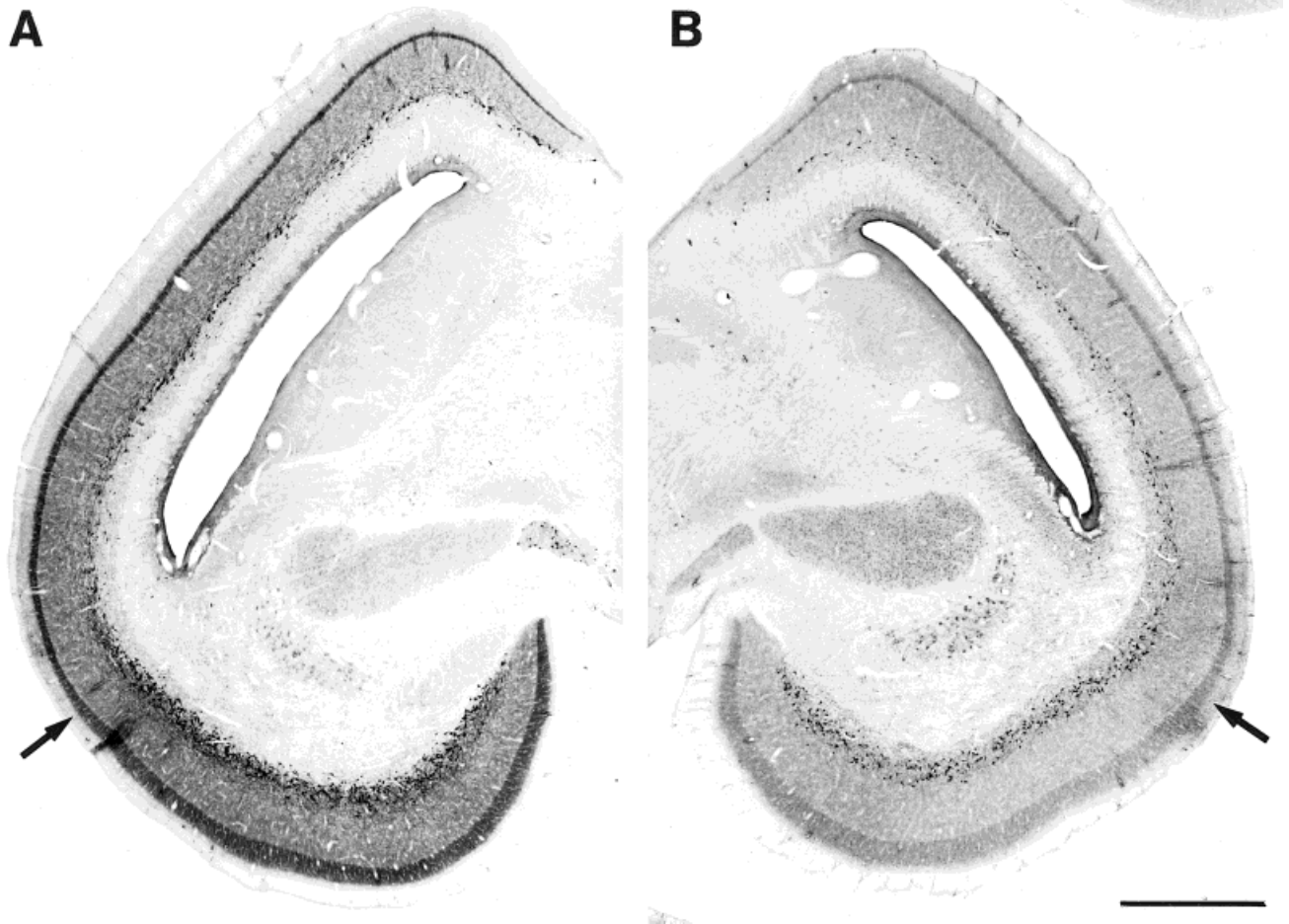


Fig. 1. Frontal sections of the left (A) and right (B) tectum opticum after a cholera toxin subunit B injection into part of the left central RT. Cell number increased from the dorsal to the ventral tectum both in the ipsi- as well as the contralateral hemisphere. Shift in soma num-

ber was paralleled by thickness variations of fiber label within layer 5b of the outer tectum. Arrows indicate a zone within the ventrolateral tectum with enhanced thickness changes of layer 5b (transition zone). Scale bar = 1,000 μm .

ventral alterations in soma distribution were determined by counting CtB-labeled cells over an extent of 920 μm within the dorsal tectum (beginning 3.5 mm dorsal to layer 5 transition zone; Fig. 1) and the ventral tectum (1.5 mm ventral to transition zone) at rostrocaudal coordinates A 2.0 and A 3.5. We were only interested in an estimation of the relative number of labeled cells between different rotundal injection sites. Therefore, no correction procedures were used. Consequently, the cell numbers reported below should not be misinterpreted as representing an absolute quantity of neurons of a certain system. Photographic documentation was carried out with a 35-mm camera-system (Olympus) attached to the microscope using Agfa APX 25 films.

RESULTS

CtB injections into nucleus rotundus (Fig. 2A) and its dorsal cap, nucleus triangularis, always resulted in a complex intrarotundal labeling pattern that never appeared spherical as would be expected from simple tracer diffusion halos. The contralateral rotundus exhibited a mirror-

like fiber label compared to the tracer diffusion within the injected rotundus (Fig. 2B).

Retrograde CtB transport resulted in bilateral labeling of tectal neurons with 64% to 71% of somata located within the ipsilateral (left) hemisphere (Figs. 1 and 3). High numbers of retrogradely labeled cells were located within layer 13 (approximately between 12,000 and 97,000 within the ipsilateral hemisphere), although, especially after tracer injections located at the outer margin of the rotundus, some additional cells could be filled in ipsilateral tectal layers 4 to 12 and 14. Surrounding structures into which tracer sometimes spread was observed included the nuclei principalis precommissuralis, ventrolateralis thalami, posteroventralis thalami, dorsolateralis posterior thalami, and dorsolateralis anterior pars lateralis. Layer 13 neurons were characterized by medium to large somata (mean area 75–240 μm^2) with multipolar, laterally to superficially oriented, primary dendritic processes that could be followed up to layer 11. Beside these correspondences, variations in rotundal/triangular injection sites caused variations in retrograde tectal labeling, pertaining to (1) soma size, their location both within (2)

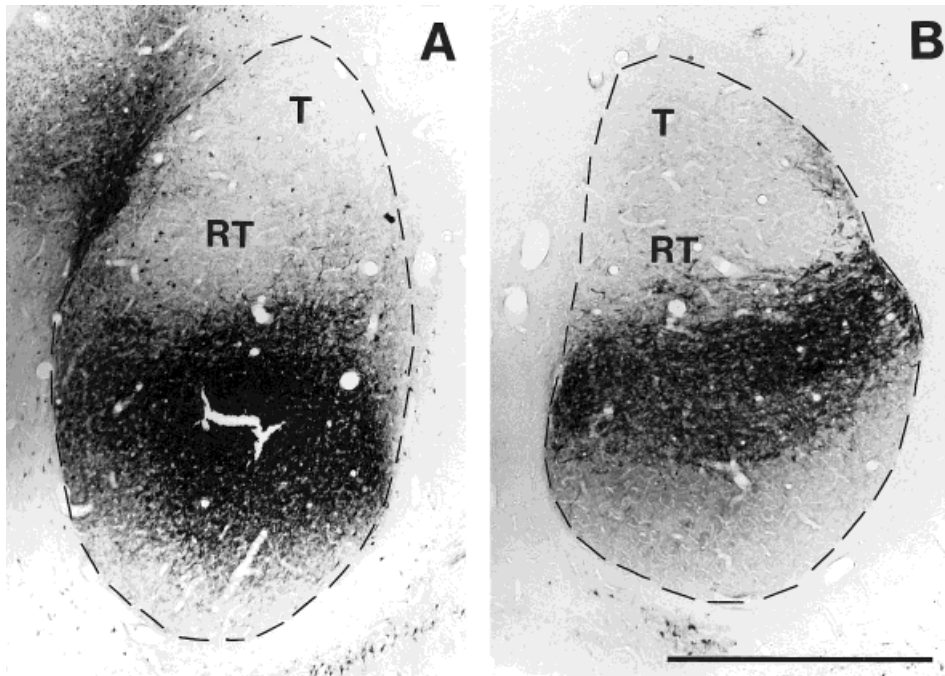


Fig. 2. Frontal sections of nucleus rotundus (RT) near cholera toxin subunit B injection site (A) and its contralateral counterpart (B) within the same pigeon. Because we observed no direct interrotundal projections, contralateral label was due to contralaterally projecting

axon collaterals of tectorotundal fibers. Thus, a given pool of tectal layer 13 neurons exhibits comparable ramifications within the rotundi of both hemispheres. T, nucleus triangularis. Scale bar = 1,000 μ m.

different layer 13 depths, and (3) their distribution over the dorsoventral extent of the tectal surface. Most obviously, (4) CtB labeling pattern varied within the outer tectal layers 3–9. Because the rotundus does not project onto the tectum (Benowitz and Karten, 1976; Nixdorf and Bischof, 1982; Karten et al., 1997; Deng and Rogers, 1998; Luksch et al., 1998), we assumed that the diffuse fiber or granular staining within the outer tectal layers was caused by CtB transport into peripheral dendritic ramifications of labeled tectal neurons. Dependent on the above four variables, we distinguished five distinct tectal labeling patterns.

The tectal *type I* pattern (Karten et al., 1997; Figs. 1 and 4, left part) was characterized by extensive, and often radially oriented ramifications with numerous local fiber swellings within layer 5b ($n = 4$). In three additional cases, a smaller number of processes also were visible in layer 5a. Type I somata were concentrated within superficial and central layer 13, with a few cell bodies also being located in deep and central layer 12. Overall, somata concentrated within the ventral tectum with three to six times more cells compared to the dorsal tectum (Figs. 1 and 5). No density alterations were observed along the rostrocaudal axis. The dorsoventral increase of cell number was paralleled by a corresponding dorsoventral increase in thickness of layer 5b label (Fig. 1). The average number of layer 13 cells (approximately 61,000) was the highest of all tectal labeling patterns. The combination of reconstructions of rotundal tracer diffusion sites ($n = 4$, Fig. 6a) revealed tectal type I labeling to be exclusively associated with CtB injections into the ventrorostral and central rotundus.

Tectal *type II* label (Karten et al., 1997) was characterized by CtB fiber tracing restricted to nonretinorecipient deeper tectal layers (layers 8–12; Fig. 4, right side). Retrogradely labeled somata (approximately 23,000 cells) were located throughout the entire depth of layer 13 with slightly more cells within the ventral optic tectum (Fig. 5). The type II pattern was exclusively observed after CtB injections restricted to the dorsalmost regions of nucleus triangularis ($n = 2$; Fig. 6).

Tectal *type III* pattern (Fig. 7, left part) was characterized by few horizontally oriented dendritic ramifications and terminal-like swellings within retinorecipient layer 4. CtB label within the retinorecipient outer tectum restricted to layer 4 was observed in only one animal with a rostral and ventrolaterally situated application (Fig. 6a). Two slightly more caudodorsally situated CtB injections resulted in additional granular label within tectal layers 5b or 5a. In the latter case, layer 5a label was restricted to the dorsal tectum, whereas its ventral regions exhibited extensive layer 4 labeling (Fig. 7, right part). Somata were located homogeneously throughout the entire depth of layer 13. Type III neurons were found with equal numbers along the dorsoventral and rostrocaudal axis of the tectum (Fig. 5A). Overall numbers of type III cells were the lowest (approximately 17,000; $n = 3$).

The tectal *type IV* pattern was characterized by extensive granular CtB label within retinorecipient layer 5a ($n = 3$; Fig. 8, left side). Additionally, the nonretinorecipient layer 8 was consistently covered by randomly oriented dendritic processes with small swellings. The type IV pattern was associated with CtB diffusion within rostrorodorsal and centromedial rotundus (Fig. 6A). Slightly more

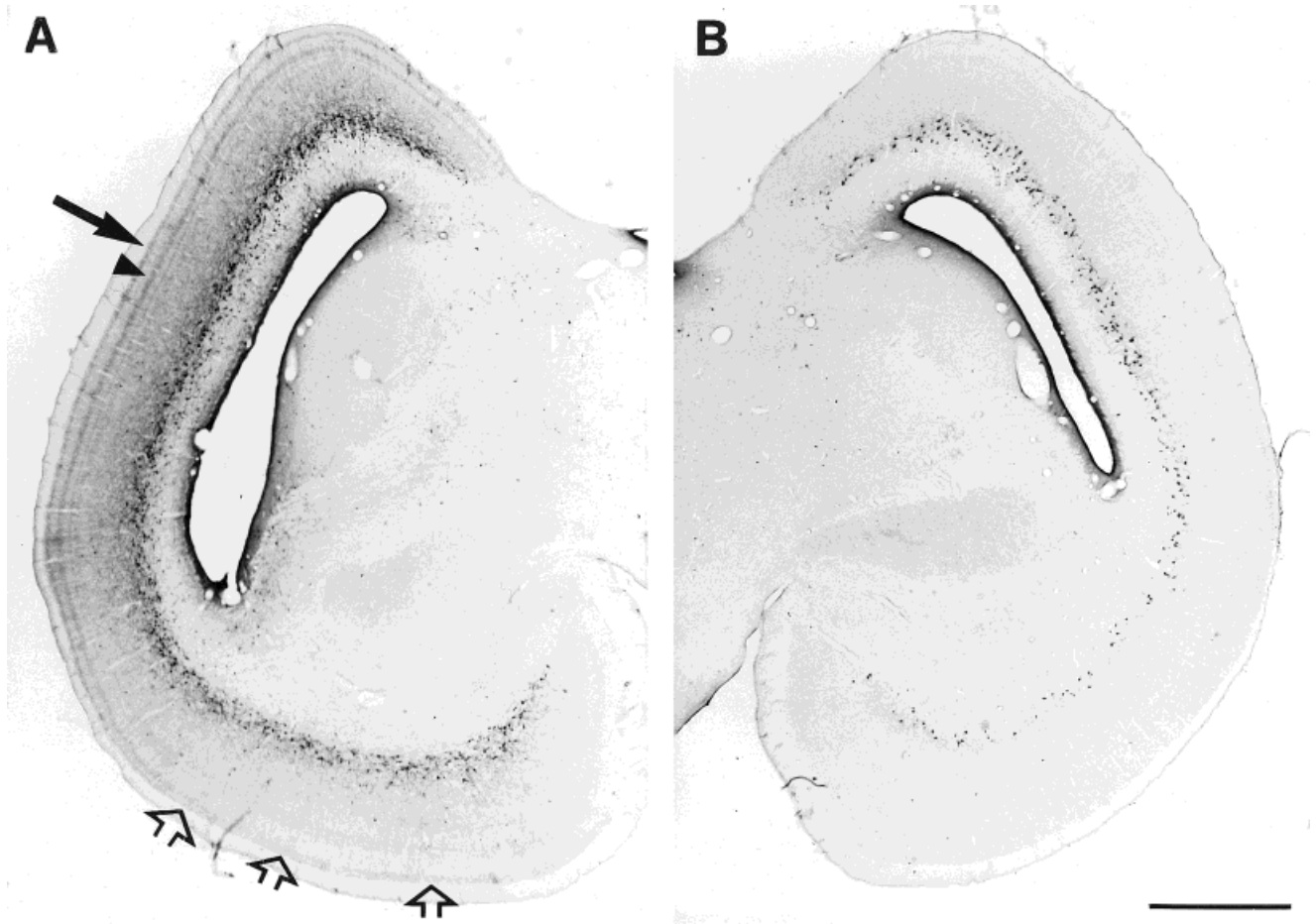


Fig. 3. Left (A) and right (B) tectum opticum after a cholera toxin subunit B injection into the left caudal rotundus. The number of cells decreased from the dorsal to the ventral tectum both in the ipsilateral and the contralateral hemisphere. Although within the dorsal ipsilat-

eral tectum fiber label is clearly distinguishable between layers 3 (arrow in A) and 5a (arrowhead in A), there is only faint and diffuse label in the outer layers 3–5a of the ventral tectum (open arrows in A). Scale bar = 1,000 μ m.

lateral/ventral tracer diffusion within the central rotundus resulted beneath strong layer 5a also in weak/substantial layer 5b CtB-like immunoreactivity (Fig. 6B). Somata (on average 41,000; $n = 5$) were concentrated within the inner and central aspects of layer 13 with approximately 1.7 times more cells within the ventral tectum, representing the inferior/frontal visual field (Fig. 5B).

Tectal *type V* labeling was characterized by CtB labeled dendritic ramifications within retinorecipient layers 3, 5a, and to a lesser extent in layer 6 ($n = 3$; Figs. 3A and 8, right side). Layer 13 somata (average cell number 38,000) clustered mainly within the dorsal tectum (two times more cells; Figs. 3A and 9B). Here the cells were located throughout the entire layer 13, whereas *type V* somata within the ventral tectum were situated at the inner margin of this lamina (Fig. 5B). Parallel to this soma distribution, *type V* label within retinorecipient layers also concentrated within the dorsal tectum. Beside this quantitative difference, a qualitative dorsoventral distinction also occurred, as the clearcut segregation of dendritic arborizations within dorsal tectal layers 3 and 5a diminished in the ventral tectum (Fig. 3A). This effect was

caused by enhanced CtB label within ventral tectal layer 4, such that the dendritic labeling covered layers 3–5a more or less homogeneously. Rotundal tracer spread in the three cases with pure *type V* labeling pattern was restricted to the caudal most rotundus (Fig. 6A). Two cases with the tracer extending into central rotundus additionally showed CtB immunoreactivity in tectal layer 5b, and was thus overlapping the *type I* labeling pattern (Fig. 6B).

Each tectal cell population was reliably labeled if tracer diffusion was restricted to certain rotundal subregions (Fig. 6A). Each of these subregions differed from each other in location, and their combination covered large regions of the rotundus. Therefore, we conclude that each layer 13 cell population projects onto separate domains of the rotundotriangular system. This does not necessarily mean that each of these layer 13 cell populations consists of a single cell type, because individual rotundal domains may receive input by more than one morphologically or physiologically specified layer 13 cell class. Indeed, our data indicate that at least the *type V* population consists of two morphologically different cell types that project commonly onto the caudal rotundal domain (see below).

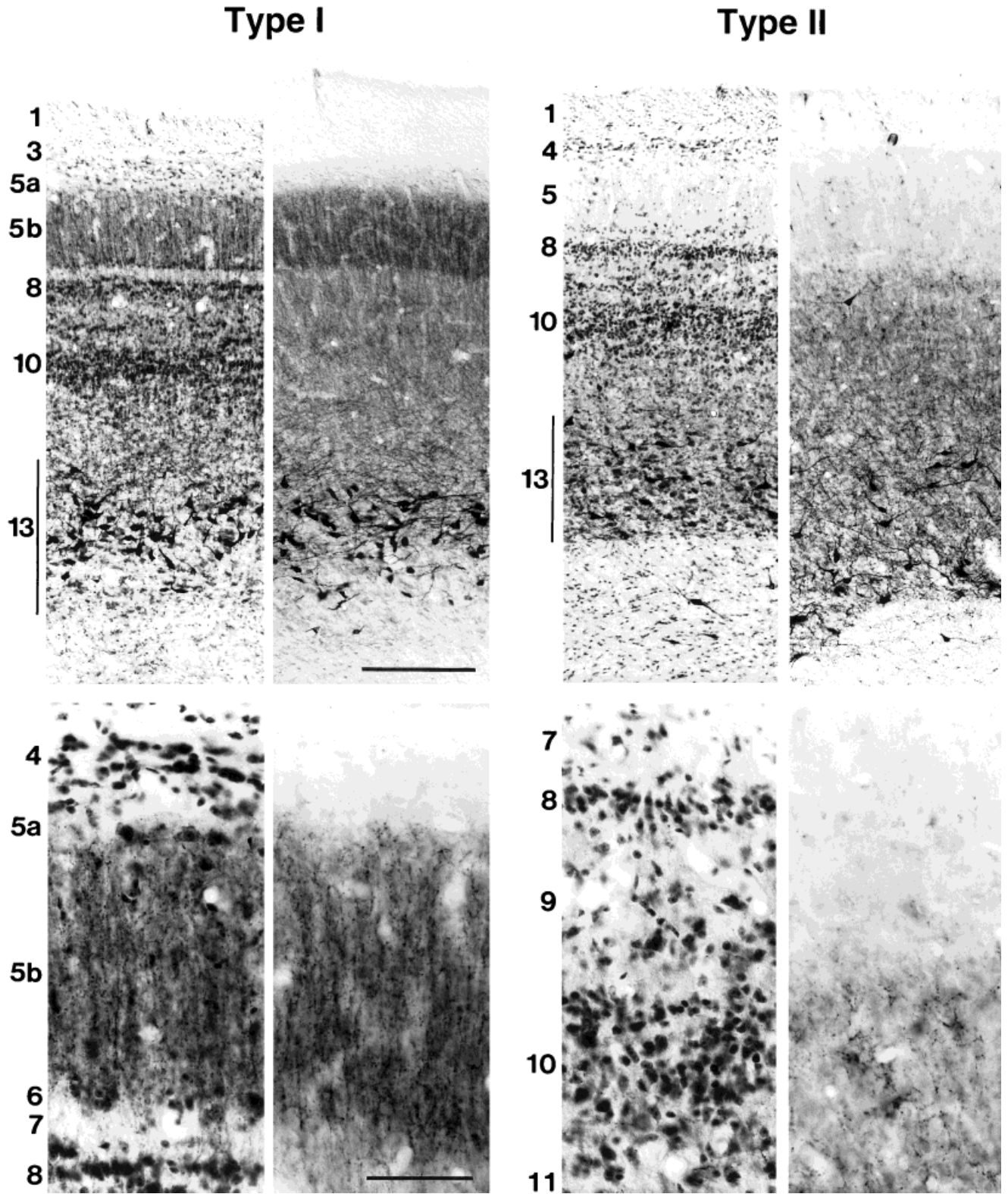


Fig. 4. Tectal type I (left) and type II labeling patterns (right). Type I somata were concentrated within the outer and central parts of layer 13. Presumably dendritic fiber labeling was concentrated within layer 5b. Within this layer, numerous radially oriented processes were visible. Type II somata were apparent throughout the entire layer 13. Fiber label spared the outer retinorecipient layers 2-7. Upper micro-

graphs: layers 1 to 14 of the lateral tectum (bar indicates 200 μ m). Lower micrographs: Higher magnification clippings of the outer (type I) respectively central (type II) tectum (bar indicates 50 μ m). Within each column left side represents combined CtB/cresyl staining, and right side portrays exactly corresponding sole CtB-label. Numbers indicate tectal laminae.

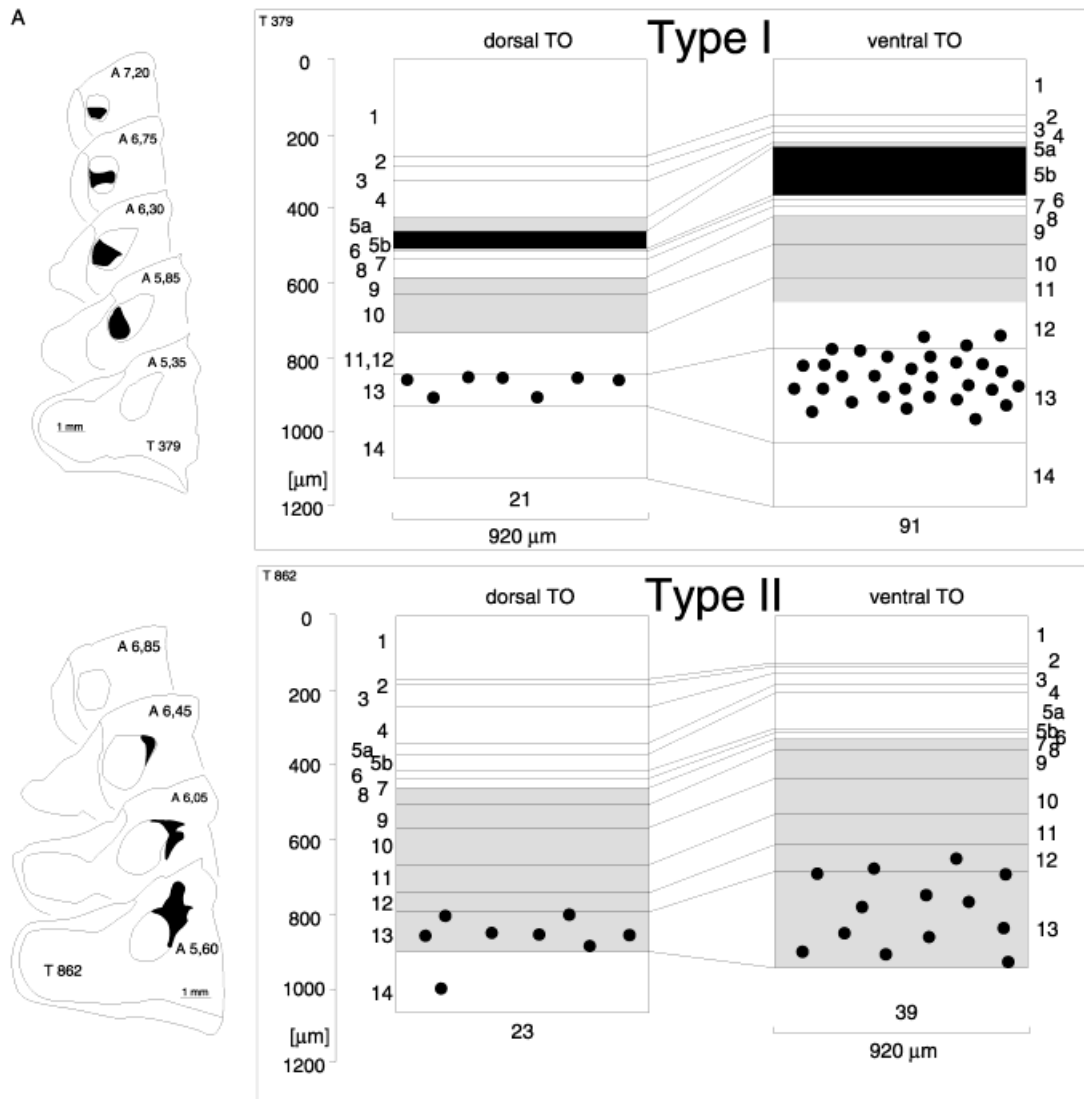


Fig. 5. Schematic reconstruction of cholera toxin subunit B (CtB) injections resulting in tectal type I–V labeling. **A:** Drawings of frontal sections, illustrating rotundal/triangular injection sites (black regions). **B:** Reconstruction of tectal labeling within the dorsal and ventral tectum (TO). Dots indicate quantitative distribution of labeled cells (see Materials and Methods section). Each dot in layers 12–14

represents approximately three neurons. Black and gray regions indicate tectal layers with high respectively low numbers (qualitative analysis) of CtB-filled thin fiber processes with presumably postsynaptic swellings. Layers with exclusive label of thick fiber processes, which probably represent fillings of stem-dendrites of layer 13 neurons, were not drawn black or gray.

Table 1 depicts the average soma sizes of retrogradely labeled layer 13 neurons for the five tectal labeling patterns. Multiple nonparametric tests on frequency distribution of soma sizes (α -corrected Kolmogorov-Smirnov test) displayed significant differences between type I and all remaining types ($P < 0.01$; $Z = 5.22$ – 6.33) as well as type V and all remaining types ($P < 0.01$; $Z = 2.41$ – 5.76), whereas no differences were displayed between types II, III, and IV ($Z = 0.56$ – 1.29). Thus, at least some of the tectorotundal neuron populations that could be differentiated by their dendritic arbors, tectal location, position within lamina 13, and intrarotundal projection area could also be distinguished by their soma size. Figure 10 displays the soma size distribution in labeling patterns I,

II–IV, and V. There is a hint of a bimodal distribution of type V. Indeed, although type V cells were found throughout the complete superficial-to-deep extent of dorsal lamina 13, the smallest neurons of this type (approximately $75 \mu\text{m}^2$) were always located at the deep margin (Fig. 11B).

Rotundal domains, characterized by their differential tectal layer 13 input, also differ in view of projections from some ipsilateral pretectal cell groups (Fig. 12). Neurons within the nTT (Deng and Rogers, 1998) were nearly exclusively filled in cases with tectal type II or V label (triangular and caudal rotundal injections; Fig. 12C). After all rotundal/triangular CtB injections, somata were labeled within the nucleus IPS, although the number of

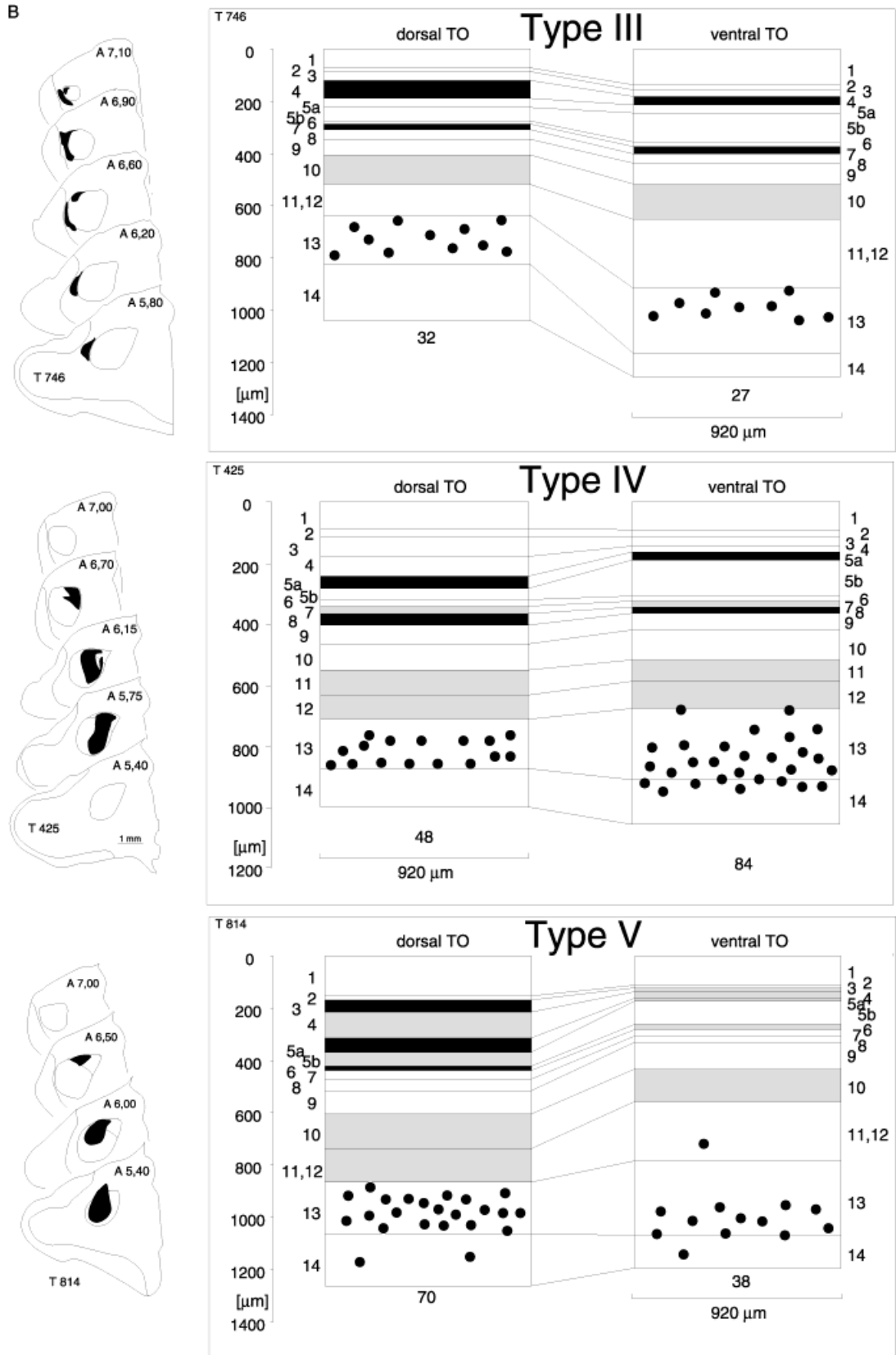


Figure 5 (Continued)

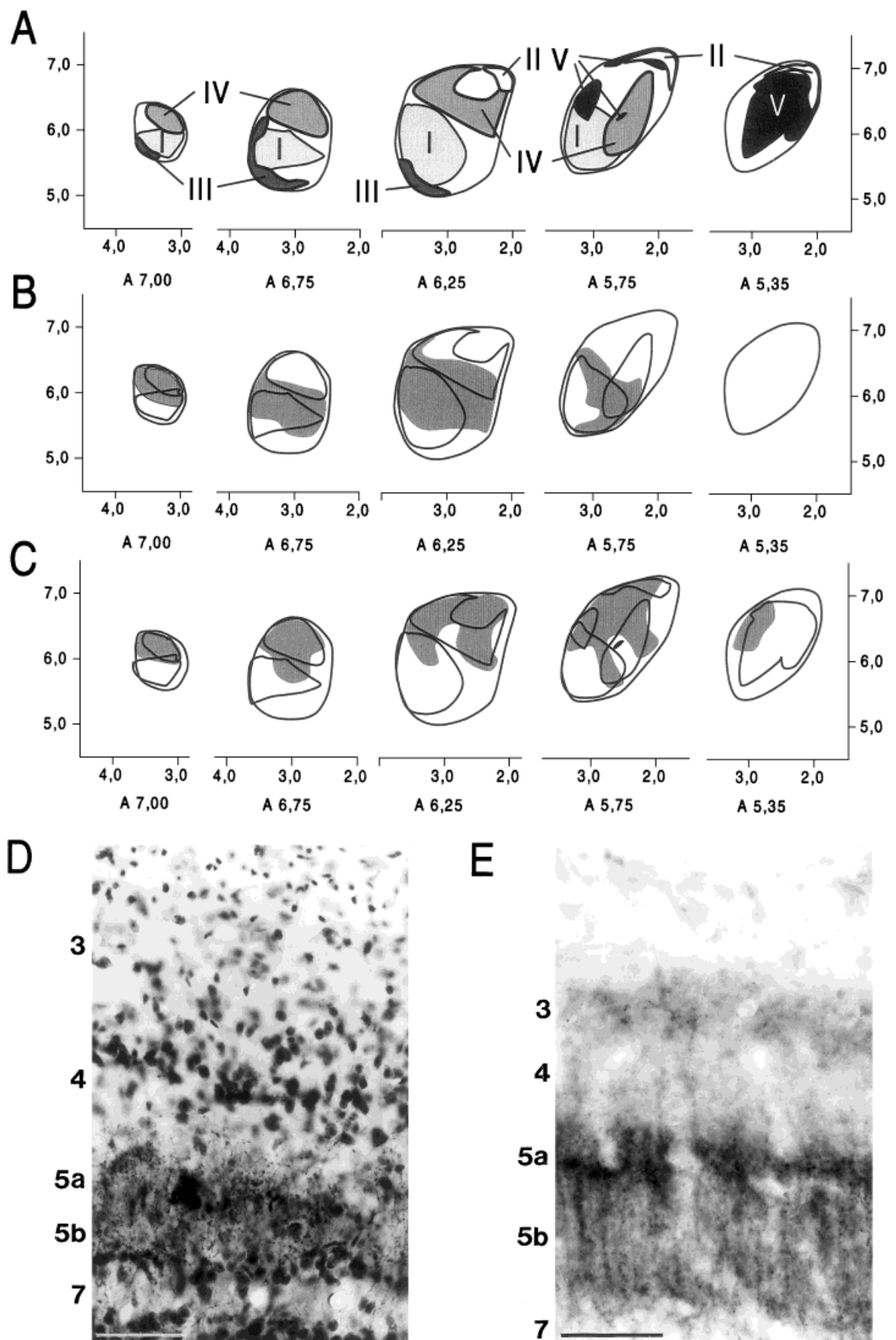


Figure 6

labeled cells was reduced after rostral rotundal injections. Cells within the dorsal components of SP were filled in cases with tectal type II, III, and V label, whereas cells within the ventral SP were traced after rostroventral CtB injections, resulting in tectal type I label (Fig. 12B). Cells throughout the entire SP were observed after more centrally situated rotundal CtB injections, resulting also in tectal type I labeling.

DISCUSSION

The present study demonstrates five morphologically distinct tectal layer 13 cell populations that together establish the tectorotundal/triangular system. These types are characterized by their location on the tectal map, the sublaminar position of their somata within layer 13, soma size, projections onto separate subregions of the nucleus rotundus or nucleus triangularis, and the differential pattern of fiber labeling within retinorecipient tectal laminae 3–7. Layer 13 neurons were already shown to exhibit dendritic ramifications within several retinorecipient layers (Ramon y Cajal, 1995; Luksch et al., 1998), where they probably contact directly optic fiber ramifications (S. Ramon cited in Ramon y Cajal, 1995; Hardy et al., 1984; Leresche et al., 1986). Golgi (Ramon y Cajal, 1995) and intracellular tracing studies (Luksch et al., 1998) demonstrated individual layer 13 neurons to exhibit dendritic ramifications over wide regions of the tectal surface. Therefore, the banded pattern of CtB labeling within different retinorecipient laminae very probably resulted from tracer transport within peripheral dendritic ramifications of retrogradely traced layer 13 cells. We will argue that the morphologic specifications of the five layer 13 cell groups establish the structural basis for spatially segregated information processing of different visual features within the tectofugal system. At the same time, we assume that these neurons constitute the transition from retinotopic to function specific coding principles that take place at the tectorotundal junction.

Spatial segregation of function

Electrophysiologic and behavioral data point to regionally segregated subareas of processing for different visual features such as color, luminance, or movement within the rotundus (Wang et al., 1993). As this organization first takes place within this structure, it is probably established by a rearrangement of the ascending visual information flow between tectum and rotundus. The present anatomical study shows that the functional segregations of the rotundotriangular system receive a differential mixture of retinal input via five tectal layer 13 cell populations and a divergent delayed inhibition via pretectal structures (see below).

Retinal ganglion cells (RGCs) can be subdivided according to morphologic and physiologic criteria into different classes, each of which subserves a different function (O'Flaherty, 1971; Mori, 1973; Ramon y Cajal, 1973; Hayes and Holden, 1980; Ehrlich et al., 1987; Karten et al., 1990; Mpodozis et al., 1995). Different classes of avian RGCs terminate in a spatially segregated manner within the tectal layers 2–7 (Ramon y Cajal, 1995; Yamagata and Sanes, 1995; Karten et al., 1997). Ultrastructural examinations have shown that these retinorecipient laminae receive at least five different types of retinal input, which are probably linked to different classes of RGCs (Repérant and Angaut, 1977). Therefore, retinorecipient laminae differ in their visual input. Thus, the four different types of layer 13 cell populations, which probably exhibit dendritic ramifications within different retinorecipient laminae, probably process different aspects of vision. Therefore, it is conceivable that the differential rotundal projection patterns of these cell groups establish the morphologic basis for segregated intrarotundal visual processing domains as shown in behavioral (Laverghetta and Shimizu, 1999) and electrophysiologic examinations (Granda and Yazulla, 1971; Jassik-Gerschenfeld and Guichard, 1972; Yazulla and Granda, 1973; Frost and DiFranco, 1976; Revzin, 1979; Wang and Frost, 1992; Wang et al., 1993). Thus, tectofugal visual information processing seems to involve parallel stimulus analysis within several functional modules, each characterized by specified sensory input by distinct classes of RGCs and subsequent processing within different layer 13 cell populations as well as regional domains of the diencephalon. Because of the topographically ordered rotundal input to the ectostriatum (Benowitz and Karten, 1976; Nixdorf and Bischof, 1982) and the topographic ectostriatal projections to subsequent regions of the forebrain (Husband and Shimizu, 1999), the structural and functional dissociations established at the tectorotundo/triangular junction should also persist at higher brain levels.

Different labeling patterns within the tectorotundo/triangular system

The organization of the tectorotundal projection in birds was the subject of numerous former studies. Most of them agree in the observation of a heterogeneous constitution of the tectorotundal projection. Dependent on rotundal tracer injection sites, retrogradely labeled layer 13 neurons were observed to vary with respect to their soma location within different layer 13 depths (Benowitz and Karten, 1976; Nixdorf and Bischof, 1982; Deng and Rogers, 1998), their dendritic ramification pattern (Karten et al., 1997; Luksch et al., 1998), and their distribution over

Fig. 6. Frontal planes of nucleus rotundus/triangularis with reconstructions of tracer injection sites, resulting in different tectal labeling patterns (I–V). The coordinate frame corresponds to the dorsoventral and mediolateral axis of the pigeon brain atlas (Karten and Hodos, 1967). **A:** Gray areas merge all regions of rotundal tracer spread in animals that exhibited pure type I ($n = 4$), type II ($n = 2$), type III ($n = 1$), type IV ($n = 3$), and type V ($n = 3$) labeling. Other cases exhibited a combination of two or more tectal labeling patterns as shown in B,C. **B:** Reconstruction of rotundal tracer spread in one animal with strong cholera toxin subunit B (CtB) labeling within tectal layers 5a and 5b (see micrograph D). The tectal labeling represents a combination of the type I and IV patterns. This is also the case for the intrarotundal CtB diffusion (gray areas) which cover wide regions of type I and IV termination areas (closed lines). **C:** Reconstruction of rotundal tracer spread in one animal with CtB labeling within tectal layers 3, 5a, and 5b (see micrograph E). The tectal labeling represents a combination of the type I, IV, and V patterns. This correlates with the intrarotundal CtB diffusion (gray areas), which combines wide regions of type I, IV, and V termination zones (closed lines). **D:** Micrograph of retrograde CtB labeling within outer tectal layers 5a and 5b (cresyl violet counterstain). Rotundal tracer diffusion is shown in B. Numbers indicate the tectal laminae. Bar represents 50 μm . **E:** Micrograph of retrograde CtB labeling within outer tectal layers 3, 5a, and 5b after a rotundal tracer injection (see C). Numbers indicate the tectal laminae. Scale bar = 50 μm .

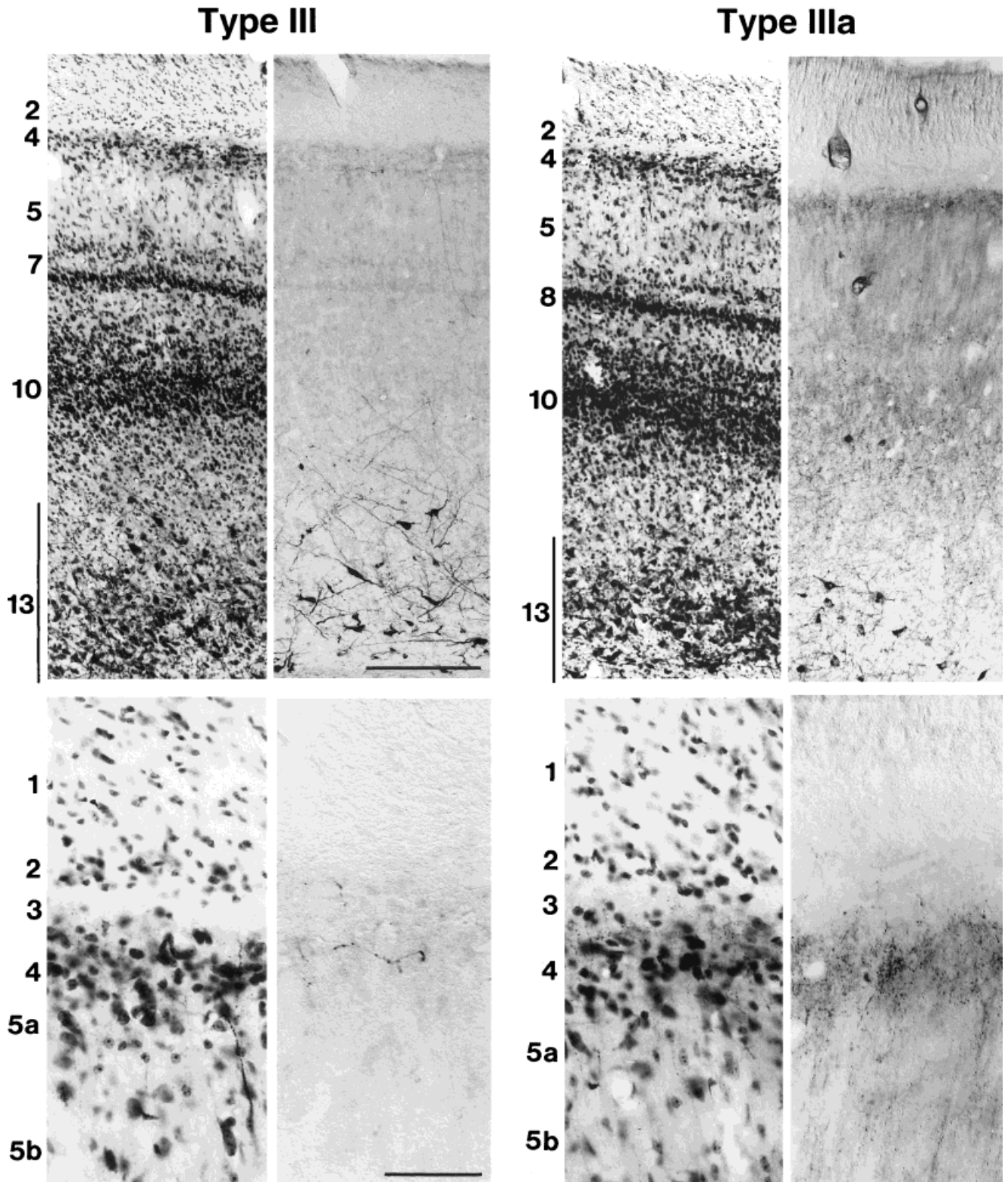


Fig. 7. Type III label within the lateral (left) and ventral tectum (right). Two different rotundal injection sites labeled somata with dendritic ramifications within retinorecipient layer 4. After cholera-toxin subunit B (CtB) injection restricted to the ventrolateral rotundus, few labeled fiber processes were filled within layers 4 and 7 throughout the entire tectum (left). In one case with a caudocentral rotundal CtB injection, relatively strong fiber label was clearly re-

stricted to layer 4 of the ventral tectum (right), whereas dorsal areas exhibited clear type V label (compare also with Figs. 3 and 8). Upper micrographs: Bar indicates 200 μm . Lower micrographs: Bar indicates 50 μm . Within each column left side represents combined CtB/cresyl staining, and right side portrays exactly corresponding sole CtB-label. Numbers indicate tectal laminae.

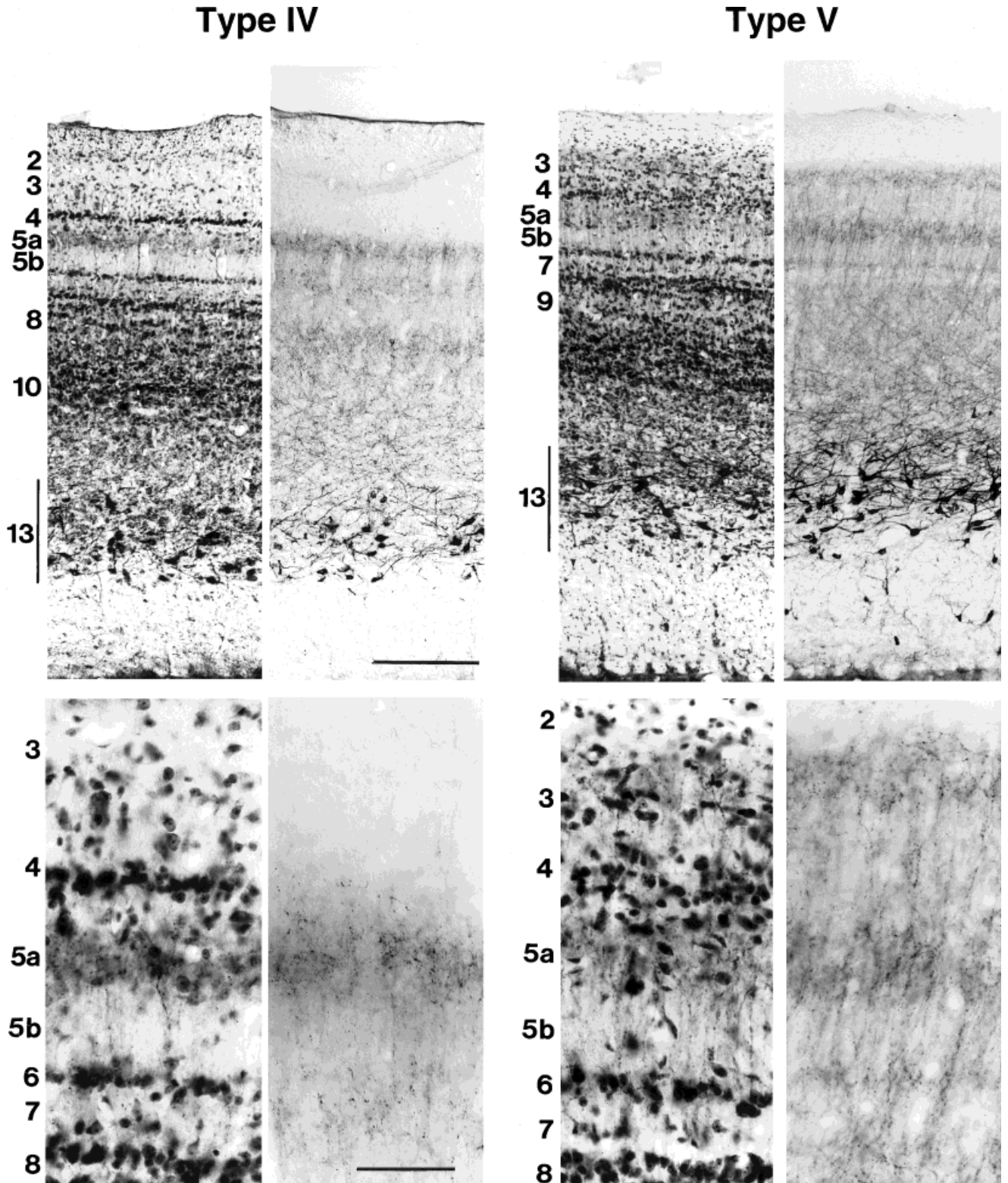


Fig. 8. Type IV (left) and type V label (right) within the lateral tectum. Dorsomedial rotundal cholera toxin subunit B injections consistently resulted in labeling tectal somata within central and deep regions of layer 13. Dendritic fiber label was concentrated within layers 5a and 8. Tracer injections into the caudalmost rotundus resulted in labeling of somata within central to deep layer 13 (dorsal tectum) or deep layer 13 (ventral tectum). Fibers within the dorsal

tectum ramified within retinorecipient laminae 3, 5a, and 6, whereas within the ventral tectum, diffuse label was obvious in layers 3-5a (compare also with Fig. 3). Upper micrographs: Bar indicates 200 μm. Lower micrographs: Bar indicates 50 μm. Within each column left side represents combined CtB/cresyl staining, and right side portrays exactly corresponding sole CtB-label. Numbers indicate tectal laminae.

the tectal map (Karten et al., 1997). Karten and coworkers (1997) were the first who categorized different types of ascending tectal layer 13 projections based on their unique connections within retinotectototundal relay. We applied and elaborated this classification of layer 13 neurons.

Type I. The type I population projects onto the rostral and central rotundus. It is characterized by extensive fiber labeling within retinorecipient sublayer 5b (Fig. 4). A comparable labeling pattern was described by Karten and coworkers (1997). An intracellular tracing study in the chicken demonstrated the characteristic widespread dendritic ramifications of individual type I neurons, with multiple radially oriented bottlebrush-like dendritic endings in layer 5b (Luksch et al., 1998). The combination of widespread dendritic ramifications and small and interspaced individual endings could constitute a morphologic basis for the ability of deep tectal as well as second-order rotundal neurons to respond to very small moving objects within large receptive fields (Jassik-Gerschenfeld et al., 1970; Frost and DiFranco, 1976; Frost and Nakayama, 1983; Wang et al., 1993; for discussion of this point see also Luksch et al., 1998). The type I population seems to be the most common and probably constitutes the largest rotundal visual processing domain. Wang and coworkers (1993) showed that nearly the entire ventral and central rotundus process motion in two-dimensional space (2d). Because extent and location of this 2d-domain matches the extent of tracer injections resulting in type I labeling, it is conceivable that this cell class participates in 2d motion analysis. Also, a second line of evidence points to an involvement of the type I population in motion processing. Based on anterograde and retrograde tracing of the retinotectal projection, Karten and coworkers (1997) concluded that tectal layer 5b receives input from small RGCs with narrow dendritic fields (w-5b type). Because this is by far the most frequent RGC type, at least within the superior retina (Karten et al., 1997), it might constitute the most frequent, movement-sensitive subtype of units within the optic tract (Maturana and Frenk, 1963; Miles, 1972; Varela et al., 1983; Mpodozis et al., 1995).

Type I neurons are four times more common within ventral tectal regions, representing the lower and frontal field of view, pointing to visual field-dependent specializations of information processing (Hamdi and Whitteridge, 1954; Jassik-Gerschenfeld and Hardy, 1984; Remy and Güntürkün, 1991; Hellmann and Güntürkün, 1999). Indeed, a recent behavioral study in pigeons could demonstrate the tectofugal pathway to be responsible for visual acuity performance mainly within the frontal, lower field of view, whereas the thalamofugal pathway guides lateral acuity (Güntürkün and Hahmann, 1999). Because the tectal type I population exhibits by far the strongest numerical enhancement within the lower/frontal visual field representation, these behavioral data indicate a contribution of type I neurons not only in 2d motion analysis but also in acuity performance and pattern recognition.

It is presently unknown how tectal neurons with wide dendritic ramifications covering substantial portions of the visual field might contribute to fine visual resolution. This problem, however, is not confined to type I. All tectorotundo/triangular cells have extensive dendritic arbors, while they respond to small moving objects (Jassik-Gerschenfeld et al., 1970; Frost and DiFranco, 1976; Frost

et al., 1990). This seems to be a common problem in many species that are capable of highly precise object localization even though the mesencephalic or telencephalic neurons involved in the sensory information processing have remarkably large, overlapping receptive fields. Hinton et al. (1986) proposed a coarse coding mechanism as a possible solution. In this model, the resolution is determined by the number of different firing patterns in the neural population as a stimulus crosses the sensory space. This results in large receptive fields yielding a high resolution as long as they overlap extensively (but not completely) and therefore show a high number of encodings (Eurich and Schwegler, 1997). If coarse coding principles also apply to the tectorotundo/triangular system, it would be conceivable how lamina 13 neurons with their wide dendritic arbors could contribute to the high visual resolution performance of the tectofugal system.

In addition to motion detection, several behavioral studies have shown the tectofugal pathway of grain-pecking birds to be also essentially responsible for pattern recognition (Hodos and Karten, 1966; Hodos and Bonbright, 1974; Macko and Hodos, 1984; Güntürkün and Hahmann, 1999), which requires high spatial resolution by, in principle, narrowly tuned receptive fields of tectal output neurons. Recent electrophysiologic work (Schmidt et al., 1999) indicates that layer 13 neurons may respond to both stationary objects within small central "hot spots" as well as to fast moving stimuli within their much larger residual receptive fields.

Type II. CtB injections into nucleus triangularis always labeled the type II subset of layer 13 neurons, characterized by dendritic ramifications restricted to nonretinorecipient layers 8–12 (Fig. 4). Because some layer 13 neurons receive not monosynaptic but disynaptic and polysynaptic retinal input (Hardy et al., 1984; Leresche et al., 1986), type II cells nevertheless might relay visual input to triangularis. An earlier study suggested that the type II neurons also project onto caudal rotundus (Karten et al., 1997)—a pattern that we could not replicate. However, the present work cannot rule out those projections, because the tectal type II labeling was restricted to the deeper tectal layers and could therefore overlap with other tectal labeling patterns without being easily distinguished. Until now, there has been no functional characterization of the triangularis, but its widespread projections onto the entire telencephalic ectostriatum, which contrasts with the topographically arranged rotundoectostriatal projection (Benowitz and Karten, 1976; Nixdorf and Bischof, 1982), might point to a modulatory role of this nucleus in tectofugal processing. Tectal input to nucleus triangularis exhibits complex regional variations, with areas receiving an extremely dense innervation from layer 13 cells of the ventral tectum, surrounded by regions with weaker dorsal tectal input (Hellmann and Güntürkün, 1999). Therefore, the modulatory role of nucleus triangularis might be related to process alterations dependent on stimulus position within the visual field.

Type III. The type III population is characterized by dendritic ramifications limited to retinorecipient layers 4 and, to a minor extent, to layer 7 (Fig. 7). Based on this characterization, a comparable cell type was shown in chicks on the basis of intracellular tracing (Luksch et al., 1998). The latter study could demonstrate that type III neurons display widespread dendritic arborizations with

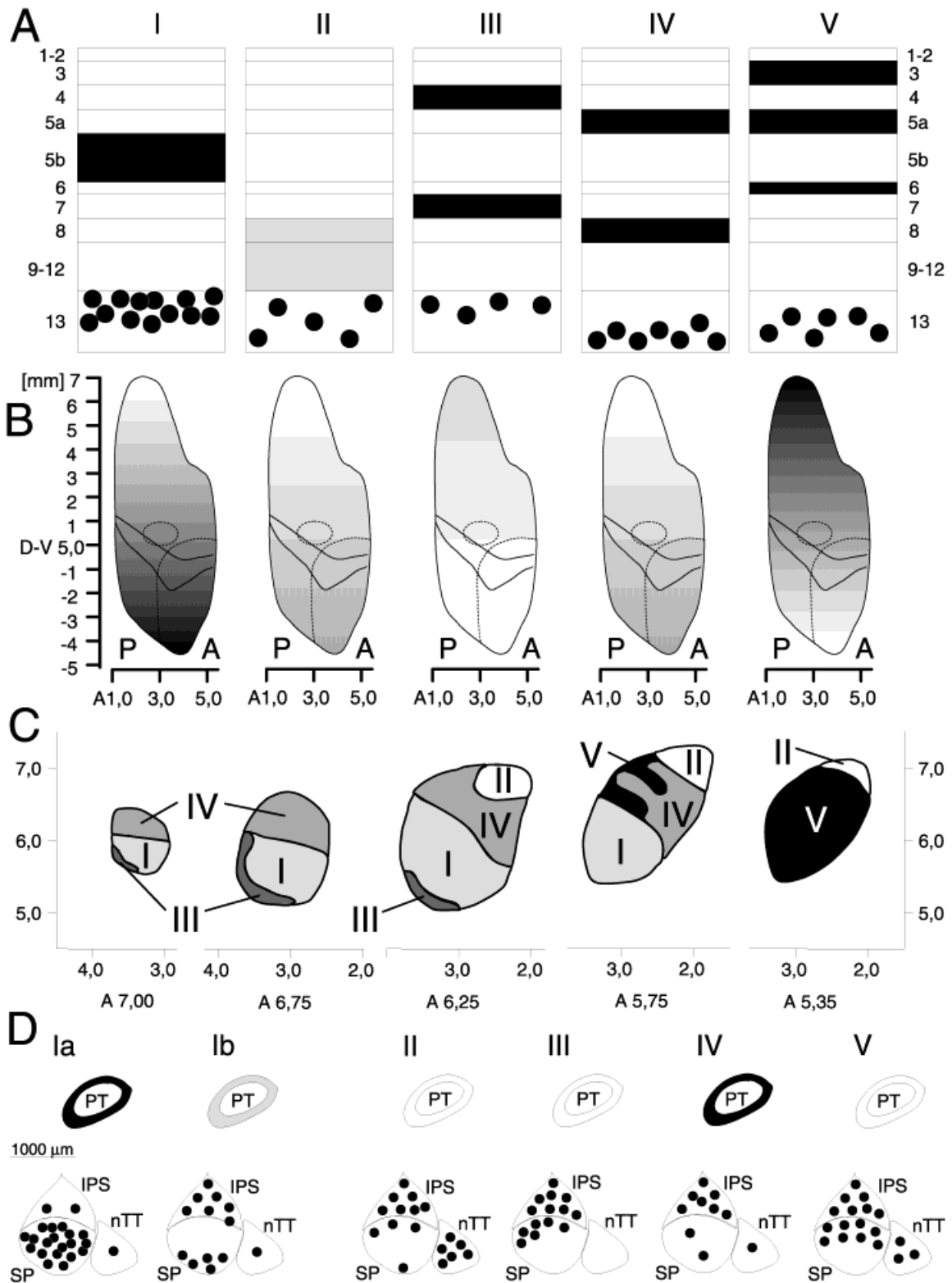


Fig. 9. Overall summary of retrograde tracing data. **A:** Different tectal labeling patterns. Roman numbers I–V indicate the five-layer 13 cell types. Black areas indicate tectal layers with high numbers of thin fiber processes presumably showing postsynaptic swellings, whereas gray areas (type II) indicate layers with comparatively few labeled thin fibers. Arabic numbers indicate tectal layers. **B:** Soma distribution over the flattened tectal surface for tectal layer 13 cell types shown above. Numbers indicate the anterior–posterior and dorsoventral position according to the pigeon brain atlas (Karten and Hodos, 1967). P, posterior; A, anterior. Intensity of gray shades correlates with the quantitative shift of soma numbers along the dorsoventral extent of the tectum (see Results section). Type I somata showed a clear peak within the ventral tectum (four times more cells)

and type V somata within the dorsal tectum (two times more cells). **C:** Different frontal planes of nucleus rotundus/triangularis with regions receiving differential tectal input. The coordinate frame corresponds to the dorsoventral and mediolateral axis of the pigeon brain atlas (Karten and Hodos, 1967). Roman numbers indicate tectal type I–V input. II indication corresponds to the extension of nucleus triangularis. **D:** Different prepectal labeling patterns. Roman numbers refer to tectal labeling. Ia and Ib: Varying prepectal soma distributions but comparable tectal type I labeling (refers to Fig. 12A,B). Nucleus prepectalis (PT) showed diffuse fiber label in most cases with tectal type I and IV label. IPS, interstitio-prepectosubprepectalis; nTT, nucleus of the tectothalamic tract; SP, nuclei subprepectalis.

TABLE 1. Summary of the Morphologic Properties of Different Tectal Layer 13 Cell Populations

Type	Position on tectal map ¹	Position within lamina 13 ²	Soma size (SD)	Dendritic arbors ³	Rotundal domain ⁴	Pretectal connectivity ⁵	Karten et al. 1997 ⁶	Luksch et al. 1998 ⁶
I	Ventral	Superficial to central	228 (10.8)	5b	Central to rostroventral	SP or IPS and ventral SP	Yes	Yes
II	Slightly ventral	Entire	167 (12.7)	8–12	Triangularis	IPS, nTT	Yes	Yes
III	Homogenous	Entire and deep	173 (2.4)	4,7	Rostroventral	IPS, dorsal SP		(Yes)
IV	Slightly ventral	Central and deep	167 (1.8)	5a,8	Dorsal	IPS		
V	Dorsal	Entire and deep	156 (4.1)	3,5a,6	Caudal	IPS, dorsal SP, nTT		

¹Position on tectal map describes the numerical distribution of cell bodies. Variations were observed along the tectal dorsoventral axis with more cells either in the ventral (types I, II, and IV) or dorsal tectum (type V).

²Position within lamina 13 summarizes the depth location of retrogradely labeled neurons (superficial = adjacent to layer 12, deep = near layer 14).

³Dendritic arbors describe the dendritic ramification patterns within the 15 layers of the tectum.

⁴Rotundal domain summarizes the presumed axonal projections onto different rotundal regions, based on the reconstruction of rotundal cholera toxin subunit B injection sites resulting in differential retrograde tectal labeling.

⁵Pretectal connectivity depicts the retrograde labeling in some pretectal nuclei (SP, nucleus subpretectalis; IPS, nucleus interstitiopretectosubpretectalis; nTT, nucleus of the tractus tectothalamicus).

⁶The last two columns compare the actual data with recent observations of divergent tectal layer 13 cell morphology in the pigeon (Karten et al., 1997) and chicken (Luksch et al., 1998).

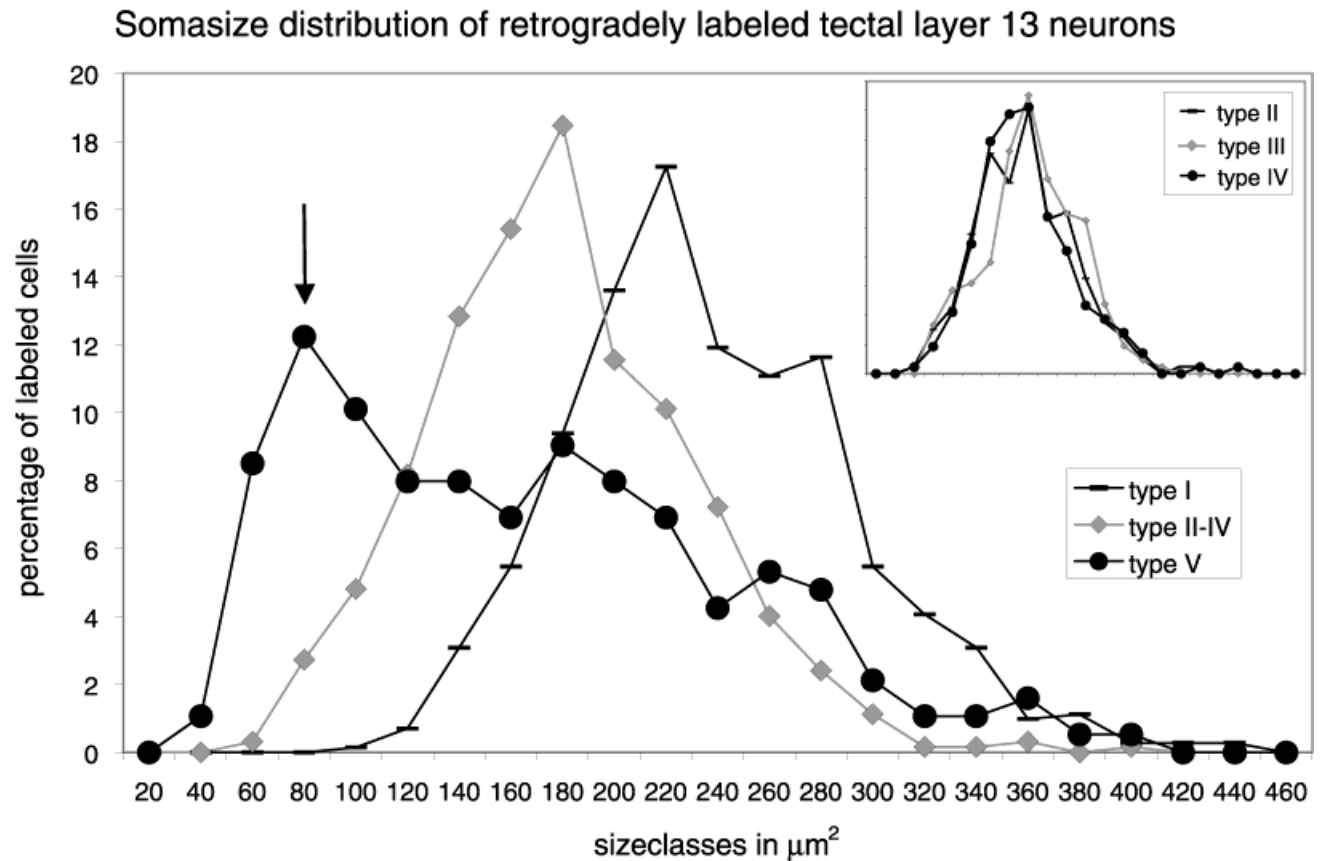


Fig. 10. Soma size diagram of different tectal layer 13 cell populations. Types I, II–IV, and V differed significantly, whereas types II, III, and IV exhibited no significant variations. Arrow points to the subgroup of small type V neurons, located at the inner margin of layer 13 (see Fig. 11B).

small, interspaced endings. Despite these similarities between pigeons and chicks, soma location and intrarotundal projection patterns of type III seem to differ between these species.

Type IV. The type IV population is characterized by dense dendritic ramifications within retinorecipient

sublayer 5a and nonretinorecipient layer 8 (Fig. 8). Thus, this newly described cell class might integrate both direct and indirect retinal input. Axonal projections of type IV neurons ramify within dorsal regions of the rostral and central rotundus, which was shown in electrophysiologic studies to be highly sensitive for color

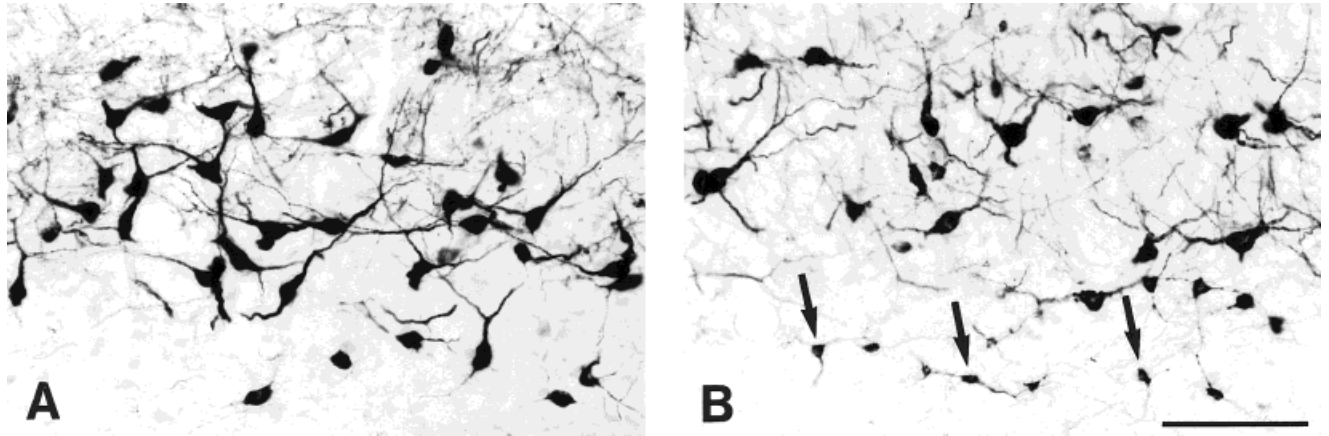


Fig. 11. Type I (A) and type V (B) cell population within layer 13 of the tectum. Note the comparatively small somata at the inner margin of layer 13 (arrows in B). Scale bar = 100 μm .

and/or luminance variations of visual stimuli (Wang et al., 1993). Karten and coworkers (1997), however, suggested that the dorsal as well as the ventral rotundus are innervated by tectal type I cells. This discrepancy may be because of the comparatively thin layer 5a labeling of type IV. Because it directly adjoins layer 5b, combined labeling patterns type I and type IV were only scarcely distinguishable from the sole type I pattern. Because type I and IV projection areas are directly adjacent, the combined pattern always occurred after dorsal rotundal CtB injections that included some additional tracer spread into the ventral subdivision. This may have caused the discrepancy between our data and the results of Karten et al. (1997).

Type V. The type V population of tectal layer 13 neurons was exclusively labeled after CtB injections into the caudalmost part of nucleus rotundus and was characterized by dense dendritic ramifications within retinorecipient layers 3, 5a, and 6. Anterograde tracing had demonstrated the caudal region as the only rotundal domain of the pigeon dominated by dorsal tectal input (Hellmann and Güntürkün, 1999). The present work confirms these data, because type V somata exhibit a twofold increase within the dorsal tectum, mapping the lateral and upper field of view. Electrophysiologic work revealed the caudal rotundus to be specialized to three-dimensional motion analysis (3d) (Wang et al., 1993), with some of these neurons especially computing time to collision for looming stimuli (Wang and Frost, 1992). If type V cells would indeed contribute to analyzing motion in 3d, their differential distribution over the tectal map might be an adaptation to looming stimuli primary emerging within the upper field of view. It is possible that the type V population can be subdivided further, because it was composed of medium-sized somata within central layer 13 and a unique very small cell group at the inner margin of layer 13. The heterogeneous constitution of type V efferents is paralleled by differential physiological properties of rotundal looming sensitive neurons, each coding a different optical variable related to image expansion (Sun and Frost, 1998).

Comparison with other morphologic studies on the subdifferentiation of nucleus rotundus

In addition to its hodologic and functional subdifferentiation, nucleus rotundus of grain-pecking birds can be subdivided on the basis of acetylcholinesterase (AChE) activity (Martinez-De-La-Torre et al., 1990), overall cell density (Theiss et al., 1998), and differential expression of various cadherins (Redies et al., 2000).

Within the rostral rotundus, the type I projection area clearly coincides with the AChE rich, relatively cell poor, and N-cadherin expressing ventrolateral (Martinez-De-La-Torre et al., 1990), respectively, anterolateral (Redies et al., 2000) portion, whereas the type IV projection zone corresponds to the AChE poor, cell rich, and N-cadherin, cadherin-6B, and cadherin-7 coexpressing anteromedial subdivision. Nucleus triangularis, receiving only type II input, exhibits general cytoarchitectonic differentiations in addition to specified AChE and cadherin expression (Benowitz and Karten, 1976; Nixdorf and Bischof, 1982). The caudal rotundus, receiving input by the type V cell population, seems to be subdivided into three small regions (intermedial, posterolateral, parafascicular) with heterogeneous AChE and calbindin expression.

Pretectorotundal system

Deng and Rogers (1998) proposed a sixfold subdivision of the tectorotundal system based on the location of tectal neurons in different layer 13 sublaminae and additionally on rotundal input from some pretectal nuclei (SP, IPS, and nTT). These nuclei receive afferents from collaterals of rotundally projecting tectal layer 13 neurons (Hunt and Künzle, 1976; Bischof and Niemann, 1990). Their ascending projections constitute the major source of inhibitory GABAergic input to the nucleus rotundus (Ngo et al., 1992; Mpodozis et al., 1996). In functional terms, Deng and Rogers' (1998) sixfold subdifferentiation defines rotundal domains, characterized by both tectal excitation (Huang et al., 1998; Theiss et al., 1998) and by delayed pretectal inhibition (Gao et al., 1995). Our data support Deng and Rogers' observations, because specific retro-

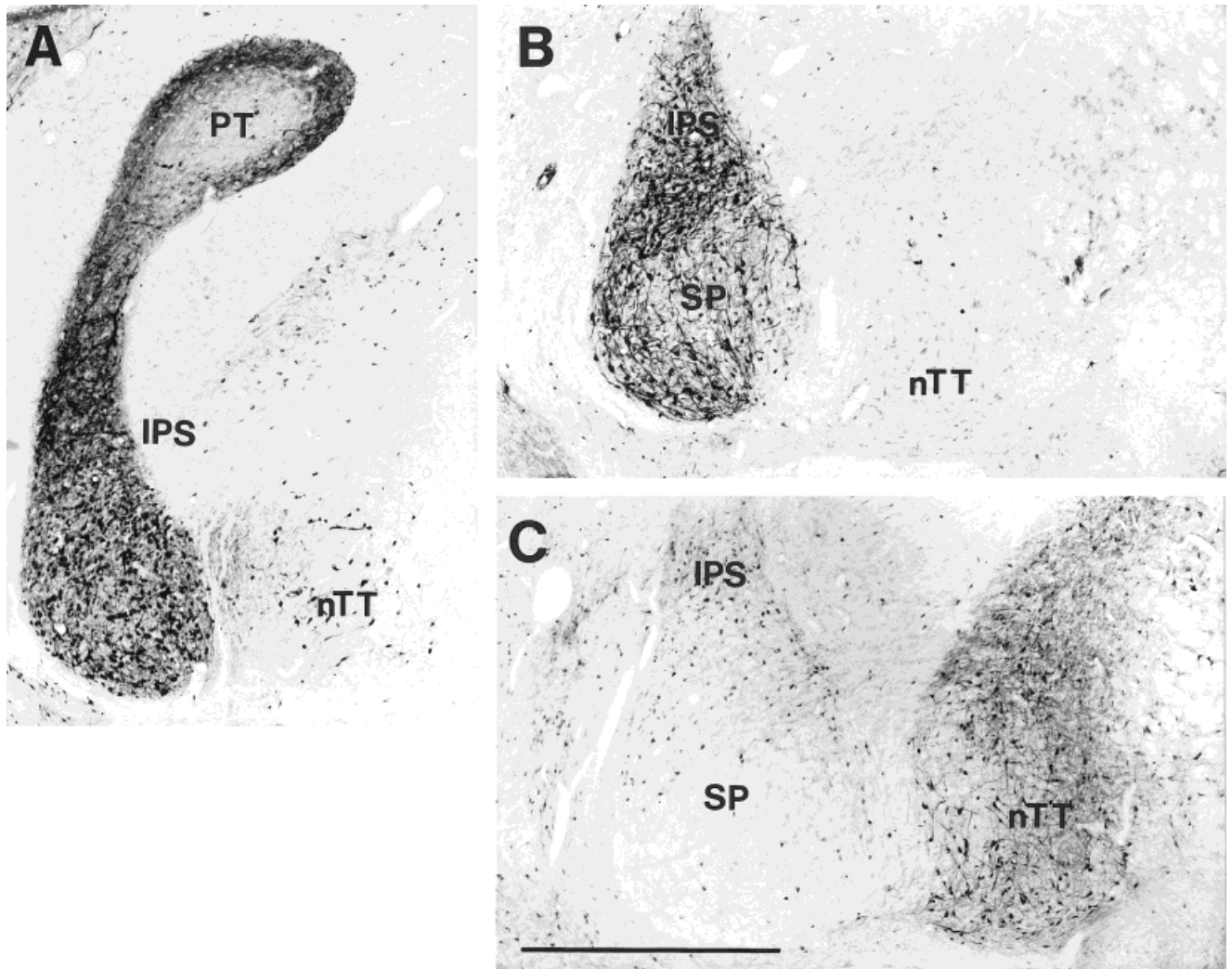


Fig. 12. Different retrograde labeling patterns within the pretectal nuclei subpretectalis (SP), interstitio-pretectosubpretectalis (IPS), and nucleus of the tectothalamic tract (nTT). **A:** Distribution of cells after a rostral rotundal cholera toxin subunit B injection. PT, nucleus pretectalis. **B:** Cells labeled after a central rotundal injection.

C: Pretectal cells after a tracer injection into nucleus triangularis (= tectal type II labeling). A+B: in both cases, tectal layer 13 neurons exhibited type I labeling, whereas pretectal somata exhibited varying distributions in different nuclei. Scale bar = 1,000 μ m.

grade labeling of type I–V neurons was accompanied by variations in labeling neurons of the SP/IPS/nTT complex (Figs. 9 and 12). Moreover, tectal type I labeling was accompanied by two different patterns of retrograde pretectal tracing (Fig. 9), suggesting a stronger rotundal regionalization than that solely based on differential tectal input.

General considerations

This study shows a complex topographic organization of the tectorotundal connection in pigeons. Each point of the tectal space map gives rise to several independent projections onto different rotundal domains, most of them matching functional specializations. Based on the fact that each point of the tectal surface gives rise to projections onto the entire nucleus rotundus, topographic place coding seems to be more or less lost at rotundal level (Benowitz and Karten, 1976; Hunt and Künzle, 1976; Nix-

dorf and Bischof, 1982; Ngo et al., 1994; Karten et al., 1997; Deng and Rogers, 1998). Conversely, behavioral studies show that the tectofugal system preserves a high degree of spatial resolution for moving as well as stationary stimuli (Hodos and Karten, 1966; Hodos and Bonbright, 1974; Macko and Hodos, 1984; Güntürkün and Hahmann, 1999). If, however, rotundal subregions receive input from divergent tectal cell types with each of them having their own unique distribution on the tectal map, it is possible that each rotundal domain preserves its own retinotopy.

In all amniotes studied so far, visual input is transferred via two pathways onto the forebrain. In birds, these are the tectofugal and thalamofugal systems, which are probably equivalent to the extrageniculocortical and geniculocortical pathways in mammals, respectively (Güntürkün, 2000). Behavioral, electrophysiologic, and anatomic data increasingly prove the existence of func-

tional segregation and parallel processing within the tectofugal visual system of birds. This also applies for the geniculocortical pathway in mammals (for review see Livingstone and Hubel, 1988). Because both systems seem to process visual features in parallel, this might be a principal feature of visual analysis at higher brain levels, probably based on the functional differentiation of RGCs, common to all tetrapodes.

ACKNOWLEDGMENTS

We thank Ariane Schwarz for excellent technical assistance, Niko Troje for critically reading the manuscript, and Martina Manns for many helpful discussions.

LITERATURE CITED

- Acheson DW, Kemplay SK, Webster KE. 1980. Quantitative analysis of optic terminal profile distribution within the pigeon optic tectum. *Neuroscience* 5:1067–1084.
- Adams JC. 1981. Heavy metal intensification of DAB-based HRP reaction product. *J Histochem Cytochem* 29:775.
- Benowitz LI, Karten HJ. 1976. Organization of tectofugal visual pathway in pigeon: retrograde transport study. *J Comp Neurol* 167:503–520.
- Bessette BB, Hodos W. 1989. Intensity, color, and pattern discrimination deficits after lesions of the core and the belt regions of the ectostriatum. *Vis Neurosci* 2:27–34.
- Bischof H-J, Niemann J. 1990. Contralateral projection of the optic tectum in the zebra finch (*Taenopygia guttata castanotis*). *Cell Tissue Res* 262:307–313.
- Deng C, Rogers LJ. 1998. Organisation of the tectorotundal and SP/IPS-rotundal projections in the chick. *J Comp Neurol* 394:171–185.
- Duff TA, Scott G, Mai R. 1981. Regional differences in pigeon optic tract, chiasm, and retino-receptive layers of optic tectum. *J Comp Neurol* 198:231–247.
- Ehrlich D, Keyser KT, Karten HJ. 1987. Distribution of substance P-like immunoreactive retinal ganglion cells and their pattern of termination in the optic tectum of chick (*Gallus gallus*). *J Comp Neurol* 266:220–233.
- Eurich CW, Schwegler H. 1997. Coarse coding: calculation of the resolution achieved by a population of large receptive field neurons. *Biol Cybern* 76:357–363.
- Eurich CW, Schwegler H, Woessler R. 1997. Coarse coding: applications to the visual system of salamanders. *Biol Cybern* 77:41–47.
- Frost BJ, DiFranco DE. 1976. Motion characteristics of single units in the pigeon optic tectum. *Vision Res* 16:1229–1234.
- Frost BJ, Nakayama K. 1983. Single visual neurons code opposing motion independent of direction. *Science* 220:744–745.
- Frost BJ, Wylie DR, Want Y-C. 1990. The processing of object and self-motion in the tectofugal and accessory optic pathway of birds. *Vision Res* 30:1677–1688.
- Gao HF, Wu GY, Frost BJ, Wang SR. 1995. Excitatory and inhibitory neurotransmitters in the nucleus rotundus of pigeons. *Vis Neurosci* 12:819–825.
- Granda AM, Yazulla S. 1971. The spectral sensitivity of single units in the nucleus rotundus of pigeon, *Columba livia*. *J Gen Physiol* 57:363–384.
- Güntürkün O, Hahmann U. 1999. Functional subdivisions of the ascending visual pathways in the pigeon. *Behav Brain Res* 98:193–201.
- Güntürkün O. 2000. Sensory physiology: vision. In: Whittow GC, editor. *Sturkie's avian physiology, fifth edition*. San Diego: Academic Press. p 1–19.
- Hamdi FA, Whitteridge D. 1954. The representation of the retina on the optic tectum of the pigeon. *Q J Exp Psychol* 39:111–119.
- Hardy O, Leresche N, Jassik-Gerschenfeld D. 1984. Postsynaptic potentials in neurons of the pigeon's optic tectum in response to afferent stimulation from the retina and other visual structures: an intracellular study. *Brain Res* 311:65–74.
- Hayes BP, Holden AL. 1980. Size classes of ganglion cells in the central yellow field of the pigeon retina. *Exp Brain Res* 39:269–275.
- Hayes BP, Webster KE. 1985. Cytoarchitectural fields and retinal termination: an axonal transport study of laminar organization in the avian optic tectum. *Neuroscience* 16:641–657.
- Hellmann B, Güntürkün O. 1999. Visual-field-specific heterogeneity within the tecto-rotundal projection of the pigeon. *Eur J Neurosci* 11:2635–2650.
- Hinton GE, McClelland JL, Rumelhart DE. 1986. Distributed representations. In: Rumelhart DE, McClelland JL, editors. *Parallel distributed processing, vol 1*. Cambridge, MA: MIT Press. p 77–109.
- Hodos W. 1969. Color-discrimination deficits after lesions of the nucleus rotundus in pigeons. *Brain Behav Evol* 2:185–200.
- Hodos W, Bonbright JC. 1974. Intensity difference thresholds in pigeons after lesions of the tectofugal and thalamofugal visual pathways. *J Comp Physiol Psychol* 87:1013–1031.
- Hodos W, Karten HJ. 1966. Brightness and pattern discrimination deficits after lesions of nucleus rotundus in the pigeon. *Exp Brain Res* 2:151–167.
- Hodos W, Macko KA, Bessette BB. 1984. Near-field acuity changes after visual system lesions in pigeons. II. Telencephalon. *Behav Brain Res* 13:15–30.
- Huang LH, Li JL, Wang SR. 1998. Glutamatergic neurotransmission from the optic tectum to the contralateral nucleus rotundus in pigeons. *Brain Behav Evol* 52:55–60.
- Hunt SP, Künzle H. 1976. Observations on the projections and intrinsic organization of the pigeon optic tectum: an autoradiographic study based on anterograde and retrograde, axonal and dendritic flow. *J Comp Neurol* 170:153–172.
- Hunt SP, Brecha N. 1984. The avian optic tectum: a synthesis of morphology and biochemistry. In: Vanegas H, editor. *Comparative neurology of the optic tectum*. New York: Plenum Press. p 619–648.
- Husband SA, Shimizu T. 1999. Efferent projections of the ectostriatum in the pigeon (*Columba livia*). *J Comp Neurol* 406:329–345.
- Jassik-Gerschenfeld D, Guichard J. 1972. Visual receptive fields of single cells in the pigeon's optic tectum. *Brain Res* 40:303–317.
- Jassik-Gerschenfeld D, Hardy O. 1984. The avian optic tectum: neurophysiology and behavioural correlations. In: Vanegas H, editor. *Comparative neurology of the optic tectum*. New York: Plenum Press. p 649–686.
- Jassik-Gerschenfeld D, Minios F, Cond-Courtine F. 1970. Receptive field properties of directionally selective units in the pigeon's optic tectum. *Brain Res* 24:407–421.
- Karten HJ, Hodos W. 1967. *A stereotaxic atlas of the brain of the pigeon*. Baltimore: Johns Hopkins Press.
- Karten HJ, Revzin AM. 1966. The afferent connections of the nucleus rotundus in the pigeon. *Brain Res* 2:368–377.
- Karten HJ, Keyser KT, Brecha N. 1990. Biochemical and morphological heterogeneity of retinal ganglion cells. In: Cohen B, Bodis-Wollner I, editors. *Vision and the brain*. New York: Raven Press. p 19–33.
- Karten HJ, Cox K, Mpodozis J. 1997. Two distinct populations of tectal neurons have unique connections within the retinotectorotundal pathway of the pigeon (*Columba livia*). *J Comp Neurol* 387:449–465.
- Laverghetta AV, Shimizu T. 1999. Visual discrimination in the pigeon (*Columba livia*): effects of selective lesions of the nucleus rotundus. *Neuroreport* 10:981–985.
- Leresche N, Hardy O, Audinat E, Jassik-Gerschenfeld D. 1986. Synaptic transmission of excitation from the retina to cells in the pigeon's optic tectum. *Brain Res* 365:138–144.
- Livingstone M, Hubel D. 1988. Segregation of form, color, movement and depth: anatomy, physiology and perception. *Science* 240:740–749.
- Luksch H, Cox K, Karten HJ. 1998. Bottlebrush dendritic endings and large dendritic fields: motion-detecting neurons in the tectofugal pathway. *J Comp Neurol* 396:399–414.
- Macko KA, Hodos W. 1984. Near-field acuity after visual system lesions in pigeons. I. Thalamus. *Behav Brain Res* 13:1–14.
- Martinez-De-La-Torre M, Martinez S, Puelles L. 1990. Acetylcholinesterase-histochemical differential staining of subdivisions within the nucleus rotundus in the chick. *Anat Embryol* 181:129–135.
- Maturana HR, Frenk S. 1963. Directional movement and horizontal edge detectors in the pigeon. *Science* 142:977–979.
- Miles FA. 1972. Centrifugal control of the avian retina. I. Receptive field properties of retinal ganglion cells. *Brain Res* 48:65–92.
- Mori S. 1973. Analysis of field response in the optic tectum of the pigeon. *Brain Res* 54:193–206.
- Mpodozis J, Letelier J-C, Concha ML, Maturana H. 1995. Conduction

- velocity groups in the retino-tectal and retino-thalamic visual pathways of the pigeon (*Columba livia*). *Intern J Neurosci* 81:123–136.
- Mpodozis J, Cox K, Shimizu T, Bischof HJ, Woodson W, Karten HJ. 1996. GABAergic inputs to the nucleus rotundus (pulvinar inferior) of the pigeon (*Columba livia*). *J Comp Neurol* 374:204–222.
- Mulvanny P. 1979. Discrimination of line orientation by visual nuclei. In: Granda AM, Maxwell JM, editors. *Neural mechanisms of behavior in the pigeon*. New York: Plenum Press. p 199–222.
- Ngo TD, Nemeth A, Tombol T. 1992. Some data on GABA-ergic innervation of nucleus rotundus in chicks. *J Hirnforsch* 33:335–355.
- Ngo TD, Davies DC, Egedi GY, Tömböl T. 1994. A phaseolus lectin anterograde tracing study of the tectorotundal projections in the domestic chick. *J Anat* 184:129–136.
- Nixdorf BE, Bischof HJ. 1982. Afferent connections of the ectostriatum and visual wulst in the zebrafinch (*Taeniopygia guttata castanotis* Gould)—an HRP study. *Brain Res* 248:9–17.
- O'Flaherty JJ. 1971. A golgi analysis of the optic tectum of the mallard duck. *J Hirnforsch* 12:389–404.
- Ramon y Cajal S. 1973. The vertebrate retina. In: Rodieck RW, editor. *The vertebrate retina: principles of structure and function*. San Francisco: Freeman. p 733–904.
- Ramon y Cajal S. 1995. *Histology of the nervous system of man and vertebrates*, vol 2. Oxford: Oxford University Press.
- Redies C, Ast M, Nakagawa S, Takeichi M, Martinez-De-La-Torre M, Puelles L. 2000. Morphological fate of diencephalic prosomeres and their subdivisions revealed by mapping cadherin expression. *J Comp Neurol* 421:481–514.
- Remy M, Güntürkün O. 1991. Retinal afferents to the tectum opticum and the n. opticus principalis thalami in the pigeon. *J Comp Neurol* 305:57–70.
- Repérant J, Angaut P. 1977. The retinotectal projections in the pigeon. An experimental optical and electron microscope study. *Neuroscience* 2:119–140.
- Revzin AM. 1979. Functional localization in the nucleus rotundus. In: Granda AM, Maxwell HJ, editors. *Neural mechanisms of behavior in the pigeon*. New York: Plenum Press. p 165–175.
- Schmidt A, Engelage J, Bischof H-J. 1999. Neurons with complex receptive fields in the deeper layers of the zebra finch optic tectum. In: Elsner N, Eysel U, editors. *Proceedings of the 1st Göttingen Conference of the German Neuroscience Society 1999*, vol 2. Stuttgart, New York: Thieme. p 470.
- Shimizu T, Karten HJ. 1993. The avian visual system and the evolution of the neocortex. In: Zeigler HP, Bischof H-J, editors. *Vision, brain and behavior in birds*. Cambridge, MA: MIT Press. p 104–114.
- Shu SY, Ju G, Fan L. 1988. The glucose oxidase-DAB-nickel method in peroxidase histochemistry of the nervous system. *Neurosci Lett* 85:169–171.
- Sun H, Frost BJ. 1998. Computation of different optical variables of looming objects in pigeon nucleus rotundus. *Nat Neurosci* 1:296–303.
- Theiss C, Hellmann B, Güntürkün O. 1998. The differential distribution of AMPA-receptor subunits in the tectofugal system of the pigeon. *Brain Res* 785:114–128.
- Vallortigara G. 1989. Behavioral asymmetries in visual learning of young chickens. *Physiol Behav* 45:797–800.
- Varela F, Letelier JC, Marin G, Maturana HR. 1983. The neurophysiology of avian color vision. *Arch Biol Med Exp* 16:291–303.
- Wang Y, Frost BJ. 1992. Time to collision is signalled by neurons in the nucleus rotundus of pigeons. *Nature* 356:236–238.
- Wang Y, Jiang S, Frost BJ. 1993. Visual processing in pigeon nucleus rotundus: luminance, color, motion, and looming subdivisions. *Vis Neurosci* 10:21–30.
- Watanabe S. 1991. Effects of ectostriatal lesions on natural concept, pseudoconcept, and artificial pattern discrimination in pigeons. *Vis Neurosci* 6:497–506.
- Yamagata M, Sanes JR. 1995. Target-independent diversification and target-specific projection of chemically defined retinal ganglion cell subsets. *Development* 121:3763–3776.
- Yazulla S, Granda AM. 1973. Opponent-color units in the thalamus of the pigeon (*Columba livia*). *Vision Res* 13:1555–1563.